Technical Physics, 2023, Vol. 68, No. 8

07

Defect-assisted tunneling via Ni/n-GaN Schottky barriers

© N.I. Bochkareva, Y.G. Shreter

Ioffe Institute, St. Petersburg, Russia
e-mail: y.shreter@mail.ioffe.ru

Received April 19, 2023
Revised May 31, 2023
Accepted June 6, 2023

Schottky barriers on GaN is considered on the basis of an analysis of the features of the current-voltage characteristics of Ni/n-GaN diodes. It is found that the forward I-V characteristics on a semilogarithmic scale have the form of curves with steps at biases corresponding to the Gaussian bands of localized states of defects in the GaN band gap. It is shown that the experimental current-voltage characteristics are in agreement with a simple physical model that takes into account the thinning of the Schottky barrier due to the space charge of ionized deep centers, which stimulates the concentration of the electric field near the Schottky contact and tunneling of electrons by hopping between local centers through the near-contact layer. At forward biases, this causes an exponential increase in the tunneling current of electrons thermally activated to an energy corresponding to the peak of the Gaussian band. The recharging of the states of the Gaussian band is accompanied by a decrease in the probability of tunneling and the appearance of a current plateau on the forward lg I(Vj) curves. An increase in the space charge of deep centers under reverse bias leads to tunneling leakage and limits the breakdown voltage.

Keywords: gallium nitride, deep centers, Gaussian impurity bands, space charge, color centers.

DOI: 10.61011/TP.2023.08.57268.101-23

Introduction

Gallium nitride and Group III nitride compounds attract attention due to their wide range of applications, including blue and ultraviolet LEDs and lasers, microwave and power transistors. GaN Schottky barriers are a key element of field-effect transistors and power diodes. Due to the high breakdown voltage and drift speed in GaN, field-effect transistors with GaN Schottky barriers are significantly superior to their silicon analogues in a number of parameters. However, the development of GaN power Schottky diodes has encountered significant difficulties, mainly related to the need to simultaneously provide a high maximum forward current density, a low reverse leakage current density, and a high electrical breakdown voltage [1–3]. Further studies are required to fully implement the benefits of the fundamental properties of GaN [1–3].

For successful practical implementation of the high potential of GaN, it is necessary, first of all, to have a more complete understanding of the transport mechanism in GaN [2] Schottky diodes. The mechanism of current flow through GaN Schottky barriers is often discussed in the literature, by analogy with crystalline silicon (c-Si), within the framework of thermoelectronic (TE), field-effect (FE) or thermal field-effect (FE/TFE) emission models [4,5]. However, many experimental facts are difficult to explain within the framework of existing concepts. Thus, in Schottky diodes with high breakdown voltage (≥ 350 V) the required forward current density $j \approx 10^2-10^3$ A/cm^2 is achieved only at voltages that are unreasonably high for Schottky barriers ($5-10$ V) [6], whereas in diodes with low maximum current density $j \approx 10^{-1}-1$ A/ cm ^{2}, saturated already at low forward voltages (0.4 V), abnormally large reverse leakage currents are observed ($j \approx 10^{-1}$ A/cm^2 already at reverse voltage $1-2$ V) and low breakdown voltage (-5 V) [7]. The reason remains unclear for the excessively large scatter in the height of the Schottky barriers (for Ni/n-GaN barriers from 0.2 [8,9] to 1.2 eV [10,11]), determined from $I-V$-measurements.

The crystalline perfection of epitaxial layers of group III nitrides is significantly inferior not only to group IV semiconductors, but also to traditional III$-$V compounds. Epitaxial layers of GaN are characterized by high density of both intrinsic and technologically inevitable impurity defects, including oxygen- and hydrogen-substituted nitrogen and gallium atoms. Defects form in the band gap of GaN a continuous distribution of localized states deeper than in amorphous hydrogenated silicon α-Si:H [12,13]. In light-emitting and photovoltaic $p-n$-nanoheterostructures, in $p-n$-homojunctions and gates of GaN field-effect transistors the deep centers created by defects facilitate tunneling through potential barriers, leading to excess tunnel currents [14–16]. However, there are few studies in the literature devoted to studying the deep centers influence on the electrical characteristics of barrier structures with unipolar conductivity, in particular, Schottky diodes [17,18].

The purpose of this paper is to identify the mechanism of influence of deep centers in GaN on electron transport in Schottky barriers using a comparative analysis of the features of the experimental $I-V$-characteristics of Ni/n-GaN Schottky diodes made on epitaxial layers and bulk GaN crystals.

1. Samples and measurement procedures

Ni/n-GaN Schottky diodes were made on the basis of Epilayers GaN of n-type conductivity with thickness $d = 1.5\,\mu$m, grown on sapphire substrates with the growth surface orientation (0001) by metal-organic compound epitaxy (metallo-organic chemical vapor deposition) (MOCVD) (diodes A and B with area 10^{-4} cm^2) and based on bulk crystals ($d = 40$ and $20\,\mu$m) grown on sapphire substrates by method of hydride vapor phase epitaxy (HVPE) (diodes C and D with area of 10^{-3} cm^2) [19]. The electron concentration in diodes A, B, C was $3 \cdot 10^{17}$ cm^{-3}, in diodes D — $2 \cdot 10^{18}$ cm^{-3} at $T = 300$ K. Ni and In were used to create Schottky contacts and ohmic contacts, respectively. Static current-voltage curve (CVC) measurements of the manufactured diodes using Keithley238 showed that all diodes provide high maximum forward current densities, reaching $j = 10^2$ A/cm^2, but differ significantly in breakdown voltage (from -5 to -180 V) and leakage current, the scatter of which reaches 5 orders of magnitude.

2. Experimental results

Figure 1 shows in semi-logarithmic scale the dependences of the current density $j(V)$ on the applied forward and reverse voltage for Schottky diodes A, B, C and D. It is obvious that all manufactured diodes have rectifying properties characteristic for Schottky barriers, but differ greatly in the breakdown voltage and leakage current. Thus, in diodes A and D (curves *1* and *4*) with the same maximum forward current density equal to $j = 10^2$ A/cm^2 at voltage $V = 2.2$ V, leakage current densities at reverse voltage $V = -5$ V differ by 5 orders of magnitude, being, respectively, $j \approx -10^{-5}$ and -2 A/cm^2. In diodes C and D (curves *3* and *4*), fast and irreversible breakdown is observed already at low reverse voltages ($V \approx -5$ V), reproducibility and the stability of the reverse $I-V$-characteristics is low. In diodes A and B (curves *1*and *2*), the reverse $I-V$-characteristics are reproducible and stable. As can be seen from the dependences presented on linear scale in the insert to Fig. 1 $j(V)$ for diodes B and A, the breakdown voltage increases to -30 and -180 V, respectively, and breakdown is observed after the reverse current density increases to $j \approx -0.2$ A/cm^2.

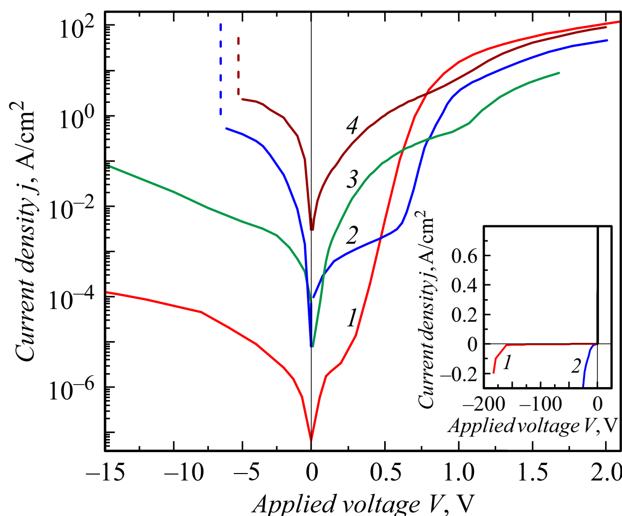

Figure 1. Current density vs. applied voltage for Ni/n-GaN Schottky diodes A, B, C and D on a semi-logarithmic scale: *1* — A, *2* — B, *3* — C, *4* — D and on the inset, diodes A, B on a linear scale: *1* — A, *2* — B.

The type of CVC of the manufactured diodes with forward bias significantly differs from the ideal Schottky diode. On the curves $\lg j(V)$ of diodes A, B, C and D, two steps are clearly visible, in which, following areas of rapid increase in current with voltage, areas of current saturation are observed. In diodes C and D (curves *3* and *4*), the forward current quickly increases already near zero bias, in the bias range $V = 0-0.2$ V, but with increasing voltage the current growth slows down, forming a plateau on the curves $\lg j(V)$ in the interval $V \approx 0.3-0.8$ V, in the region of which the current density does not exceed $j \approx 1-10$ A/cm^2. In the literature, a similar feature of CVC of GaN Schottky diodes is often associated with the low height of the Schottky barrier, equal to ~ 0.2 eV, and the limitation of the current by the spreading resistance and the resistance of the ohmic contact. However, estimates of the value of series resistance r_s from experimental $I-V$-characteristics give for r_s an unjustifiably large value ($\sim 10^3-10^4\,\Omega$), indicating the dominance of another mechanism of charge carrier transport through Schottky barriers. Moreover, following the plateau on the curves $\lg j(V)$, a stepwise increase in the current is again observed up to the current density $j = 10^2$ A/cm^2 at direct voltages not below $V = 2.2$ V, which are abnormally high for Schottky barriers.

GaN Schottky diodes are characterized by the absence of a linear section of $I-V$-characteristics at high forward voltages, usually observed in Schottky diodes when approaching the flat band voltage V_{fb} and determined by the value of the series resistance of diode. To estimate the magnitude of the decrease in the height of the Schottky barrier by the applied forward voltage, the series resistance of the diode was taken equal to the differential resistance $r_s = dV/dI$ at maximum current and for diodes A, B, C and D was 417, 53, 59 and 9.5 Ω respectively. The obtained dependences of the forward current density on the forward bias of the Schottky barrier (potential energy of electrons at the Fermi level F), measured in energy units (electron volts), $V_j = q(V - I \cdot r_s)$ (q — elementary charge, I — forward current), for diodes A, B, C and D are presented in Fig. 2, curves *1*–*4*. Comparison of dependencies $j(V_j)$ (curves *1*–*4*) and $j(V)$ (curves 1^*–4^*) shows that for $V > 1$ V, virtually all applied voltage drops across the series resistance rather than across Schottky barrier. In the region of high current densities $\sim 10^2$ A/cm^2 the slope of the curves $j(V_j)$ increases with bias increasing, the curves $j(V_j)$, as well as the curves $d_j/d\,V_j(V_j)$ (shown

in section 3) in all diodes asymptotically approach the vertical at almost the same forward voltage V_j/q on the Schottky barrier, which can be taken as the flat band voltage $V_{fb} = V_0/q$. For diodes A, B, C and D, the scatter of the forward bias value at which the curves $j(V_j)$ and $d_j/dV_j(V_j)$ approach the vertical is found in the interval $V_j = 1.14-1.17$ eV, which corresponds to the height of the Schottky barrier $V_0 = 1.1-1.2$ eV and is consistent with the data obtained for the height of Ni/n-GaN barrier in papers [10,11].

3. Discussion of results

3.1. Tunneling through localized states in the forward direction

View of $\lg j-V$-characteristics for forward bias of diodes A and B with extended exponential sections in the region of average biases (Fig. 1, curves *1*, *2*) is typical for GaN Schottky diodes with maximum forward current density reaching $\sim 10^2$ A/cm^2, and is usually described in the literature by the well-known empirical formula:

$$I = I_0(V)\exp(qV/nkT), \quad (1)$$

where kT/q — thermal potential, $I_0(V)$ — saturation current, parameter $n(V)$ — perfection factor. By analogy with crystalline Si, the value of the perfection factor $n(V)$ is used to judge the predominant mechanism of the current flowing through the barrier. When $2 > n > 1$, the total current is considered as the sum of two components of comparable magnitude: the thermionic current, characterized by the perfection factor $n = 1$, and the recombination current, for which $n = 2$. The perfection factor $n > 2$ is interpreted as the dominance of the tunnel current. An exponential increase in current in the region of medium voltages, characterized by the perfection factor close to unity, is usually associated with the dominance of the above-barrier thermionic current, a subsequent decrease in the slope of the curve $\lg j(V_j)$ with voltage increasing — with voltage drop across the series resistance of diode. But the behavior of the current with the increasing of forward bias and $j(V_j)$-characteristics of the studied Schottky diodes contradicts these ideas.

As can be seen from Fig. 2, $\lg j-V_j$-characteristics of diodes A and B (curves *1*and *2*) in the region of average biases have sections characterized by the perfection factor close to unity ($n = 1.2-1.3$). But with increasing bias on the curves $\lg j(V_j)$, a plateau is observed in the range of biases $V_j \approx 0.8-1$ eV, in the region of which $n \geq 4$, and then the perfection factor decreases again to a value close to unity near the bias $V_j = 1.12$ eV. In the region of small biases in the curves $\lg j(V_j)$, a shoulder is observed, the plateau of which extends in diodes A and B to 0.2 and 0.6 eV, respectively, and in diodes C and D up to 0.8 and 1 eV respectively.

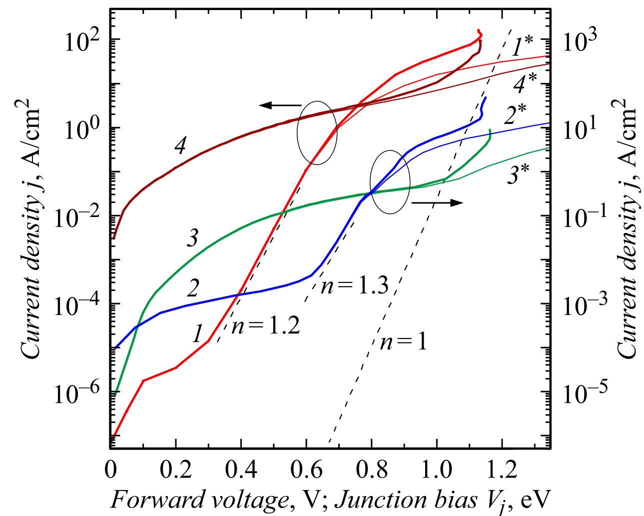

Figure 2. Current density vs. forward voltage (*1**–*4**) and vs. forward bias of the Schottky barrier (*1* –*4*) for Ni/n-GaN diodes A, B, C and D. *1**, *1* — A; *2**, *2* — B; *3**, *3* — C; *4**, *4* — D. The dashed lines illustrate the dependences of the forward current $j(V_j) \propto \exp(qV_j/nkT)$ for $n = 1.2$, 1.3 and 1.

If we assume that a sharp increase in current near the voltage of flat zones is associated with the flow of above-barrier thermionic current, then, as can be seen from Fig. 2, for all diodes the current in the region of average biases by more than 3 orders of magnitude is higher than the above-barrier thermionic current. This indicates that the effective height of the potential barrier is reduced due to electron tunneling under the barrier. Moreover, in contrast to the interpretation of the empirical formula (1) established in the literature, the tunneling excess current in diodes A and B is characterized by the perfection factor close to $n = 1$. This also allows us to consider the $I-V_j$-characteristics under forward bias as current tunnel spectra, the shape of which, like Esaki tunnel junctions, reflects the energy distribution of deep centers in the band gap [20] .

3.2. Tunneling spectroscopy of deep centers

According to the data of photoluminescence, optical absorption and photoionization spectroscopy, the deep quasi-continuous distribution of localized states in the band gap of GaN can be represented as a superposition of impurity Urbach tails of the density of states of the conduction band and valence band and Gaussian bands of localized states of defects — color centers forming impurity zones in the upper and lower halves of the band gap of GaN and responsible for the broad, partially overlapping bands of yellow, green, blue and UV intracenter photoluminescence (PL) (YL, GL, BL and UVL bands, respectively) and intracenter optical absorption (the full width of the bands at half height, FWHM≈ 0.4 eV) [12,13,21–28].

In epitaxial GaN layers the high density of local centers allows electrons to tunnel by hopping between

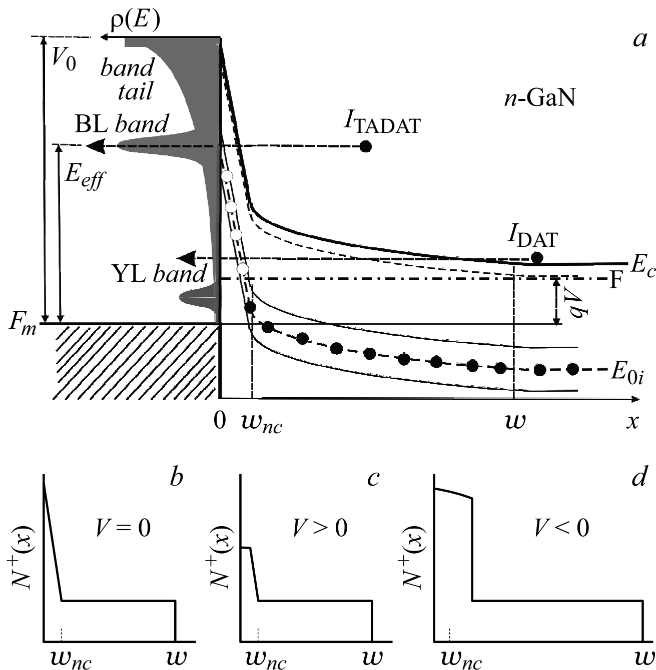

Figure 3. a — schematic illustration (on the diagram „one-electron energy E — coordinate X“) model of tunneling in barrier metal — n-GaN through SCR with width w, taking into account the increase in the built-in electric field in the near-contact layer of thickness w_{nc} by ionized deep centers. The energy spectrum of defects $\rho(E)$ is graphically illustrated, it corresponds to the case of dominance of the Gaussian band of BL-centers band (BL-band) with a maximum E_{0i} over the band of YL-centers (YL-band) and Urbach tail of states (band tail) in the tunnel spectra $j(V_j)$ and $g_{tun}(V_j)$ of diodes Ni/n-GaN A and B, presented in Fig. 2 and 4, curves *1, 2*. The main tunnel current I_{TADAT} flows along the tunnel transport layer $E_t = E_{0i}(x = 0)$, through the effective barrier of height $E_{\text{eff}} = E_{0i}(x = 0)$ and dominates the current I_{DAT} of electrons, tunneling from states at the bottom of the conduction band in the bulk of GaN; *b,c,d* — charge density distribution in SCR at $V = 0$, $V > 0$, $V < 0$.

centers. Hopping conductivity through weakly localized states makes a significant contribution to electron transport already at room temperature, and with temperature decreasing the conductivity decreases only by 1−2 orders [29]. During optical injection electrons are thermalized with the participation of phonons by hopping from shallow states to deeper ones, and the hopping current is transferred along the transport level, for which the rates of electron thermalization to deeper states and thermal excitation to shallower states are equal [30,31].

In barrier metal/n-GaN (Schottky) at forward voltage V the tunnel flow of electrons with energies E in the interval $V_0 > E \geq F$ (V_0 — potential energy of the electron at the top of the barrier relative to the Fermi level of the metal F_m; $F(x = w) = F_m + qV$ — Fermi level in neutral region of GaN) moves from the conduction band to the Schottky interface through the space charge region (SCR) with a full width w due to hopping diffusion near tunnel transport levels horizontal in energy $E_t = E$, tunneling „under“ the top of the barrier by hoppimg from shallower states to deeper ones. Schematically, the process of tunneling through the SCR of the contact metal/n-GaN along localized states with density $\rho(E)$ in the band gap of GaN is shown in Fig. 3, *a*. The rate of tunneling transfer of electrons through the SCR is limited by a near-contact layer of thickness w_{nc} with the highest localization energy and the lowest density of local centers along the tunneling length.

The current created by tunneling transitions of electrons is proportional to the product of the density of electron-filled initial states $\rho_s(E_t)$, the total density of empty final states of the impurity band $\rho_{Gf}(E_t)$ and the Urbach tail $\rho_{Uf}(E_t)$ on tunnel transport level E_t in the near-contact layer w_{nc} and the probability of tunneling through the near-contact layer $D(E_t)$ (tunnel permeability of the barrier) [32]:

$$I(E_t) \propto \rho_s(E_t)(\rho_{Gf}(E_t) + \rho_{Uf}(E_t))D(E_t). \qquad (2)$$

The probability of tunneling through a triangular potential barrier in its simplest form is [33]:

$$D = \exp\left(-\frac{\pi}{2\sqrt{2}}\sqrt{2m^*(V_0 - V_j)} \cdot \frac{\delta}{\hbar}\right), \qquad (3)$$

where V_0 and $\delta = (V_0 - V_j)/qF_b$ — barrier height and width, V_j — forward bias ($V_j < V_0$), $F_b = ((V_0 - V_j)N^+/\varepsilon\varepsilon_0)^{1/2}$ — electric field strength, q — elementary charge, ε_0 — electric constant, ε — relative dielectric constant, $1/m^* = 1/m_e + 1/m_h$, m_e and m_h — effective electron and hole masses, m^* — reduced effective mass of electron and hole, $N^+ = N_d + N_U^+ + N_G^+$ — total concentration of shallow donors N_d, ionized deep centers of the Urbach tail N_U^+ and Gaussian impurity bands $N_G^+ = \sum_i N_{Gi}^+$.

In the case of $N_U^+ \gg N_G^+$ and the dominance of Urbach tail centers in the total volume charge over the centers of Gaussian impurity bands, the main contribution to the tunneling current is created by electrons with energies near the energy of the bottom of the conduction band $E_c(x = w)$, counted from the Fermi level of the metal F_m, (current I_{DAT} (defect-assisted tunneling, DAT) in Fig. 3, a), tunneling near the transport level $E_t = E_c(x = w)$, since at the Urbach energy $E_U > kT$ the electron density at the level $E_t > E_c(x = w)$ decreases with increasing energy V_j faster than the density increases of localized states of the Urbach tail.

In the case of $N_{Gi}^+ \gg N_U^+$ and dominance in the total bulk charge of centers of i-th Gaussian band over the centers of the Urbach tail, the main current is created by electrons thermally activated at the top of the effective barrier E_{eff} (current I_{TADAT} (thermally activated defect-assisted tunneling) in Fig. 3, *a*), and flows near the transport level $E_t = E_{\text{eff}}$, where the effective barrier height E_{eff}, measured from the Fermi level of the metal F_m, is decreased due to tunneling to the energy at the maximum of the Gaussian of ith impurity band at the Schottky interface: $E_{0i}(x = 0) = E_{\text{eff}}$. Since the

concentration of carriers capable of overcoming the effective barrier is determined by the Boltzmann distribution, the differential resistance of the barrier SCR is inversely proportional to the current and is equal to $r_{\text{eff}} = kT/qI$. At low currents r_{eff} is greater than the series differential tunnel resistance of the near-contact layer r_{tun}. The forward voltage increment drops almost entirely at the effective barrier, lowering its height and leading to the exponential increase in the tunneling current with voltage, characterized by the perfection factor $n = 1$. As the forward current increases, the resistance r_{eff} decreases, and the major part of the bias increment falls on the tunnel resistance r_{tun}, straightening the zones predominantly near the Schottky interface, which slows down the decrease in the effective barrier with bias increasing, and leads to increase in the perfection factor.

The shape of the current tunneling spectra of barrier structures is usually analyzed using the Esaki deep center tunneling spectroscopy method [20] and modified tunneling models based on the Esaki approach [34]. The analysis is based on the assumption that the width of the barrier SCR is determined by the concentration of the main dopant, and the shape of the tunnel spectra reflects the energy distribution of the deep centers density in the band gap.

Analysis of the discovered features of the tunnel current behavior with forward bias increasing allows us to conclude that deep centers, ionized during screening of the field of the contact potential difference, make a significant contribution to the value of the space charge density in the SCR of the Schottky barrier (Fig. 3, *b*). This leads to a concentration of the built-in electric field at the Schottky contact and thinning of the Schottky barrier, which, in turn, leads to an increase in the tunneling probability (3) and tunneling conductivity of the barrier $g_{tun}(E_t)$ (2). In this case, the nature of the energy distribution of deep centers in the band gap determines the nature of the spatial distribution of localized states along the levels $E_t = E_c(x = w)$ and $E_t = E_{\text{eff}}$ during forward bias.

As the tunnel transport level $E_t = E_c(x = w)$ with increase in forward bias moves up along the energy scale to the top of the barrier and crosses the impurity Gaussian bands, the ionized deep centers are filled with electrons, and the bulk charge density in the near-contact layer decreases (Fig. 3, *c*), leading to decrease in its tunnel permeability. Since almost the entire increment of forward voltage drops at the near-contact layer, the density of initial states filled with electrons $\rho_s(E_t)$ at the tunnel transport level E_t at $x = w_{nc}$ increases relatively weakly with bias increasing. In this case, according to (2) the dependence of the differential tunnel conductivity of the barrier $g_{tun}(E_t) = dI(E_t)/dE_t$ on the density of empty final states of the impurity band $\rho_{Gf}(E_t)$ and the Urbach tail $\rho_{Uf}(E_t)$ at the level E_t becomes nonlinear:

$$g_{tun}(E_t) \propto D(E_t)\left(\frac{d\rho_{Gf}}{dE_t} + \frac{d\rho_{Uf}}{dE_t}\right) + (\rho_{Gf} + \rho_{Uf})\frac{dD(E_t)}{dE_t}. \quad (4)$$

In the case where the density of states of the Gaussian band $(d\rho_{Gf}/dE_t \gg d\rho_{Uf}/dE_t)$ predominates in the GaN band gap in the energy range probed by the level E_t, the growth rate of the density of empty states participating in tunneling $d\rho_{Gf}/dE_t$ at the transport level, which moves upward with increase in bias, quickly increases at the edge of the zone and slows down to zero when approaching the maximum of the Gaussian, which leads to the appearance of convexity in the curve $\lg g_{tun}(V_j)$. At the same time, the rate of filling the band states and decreasing the bulk charge density becomes maximum at the maximum of the Gaussian, leading to decrease in the tunneling probability, which, in turn, compensates for the increase of $\rho_{Uf}(E_t)$ at the level E_t with bias increasing, leading to the appearance of a plateau on CVC, and increase in the contribution of the tunnel resistance r_{tun} to the series resistance of the diode r_s.

3.3. Tunneling spectroscopy of deep centers in Schottky barrier

From the dependences of the differential conductivity of diodes A, B, C and D on the forward bias of the Schottky barrier presented in Fig. 4, it is clear that the diodes exhibit a strong scatter in the conductivity g_{tun} near zero bias and significantly smaller ones as the bias approaches $V_j = 1.2$ eV, and the main increase in g_{tun} occurs in two bias intervals, $V_j = 0-0.6$ eV and $0.6-1.2$ eV. But the nature of the growth g_{tun} in these intervals for diodes A and B and for diodes C and D is opposite. Thus, at small biases $V_j < 0.6$ eV the tunnel conductivity g_{tun} of diodes C and D is much greater than that of diodes A and B, but as the bias

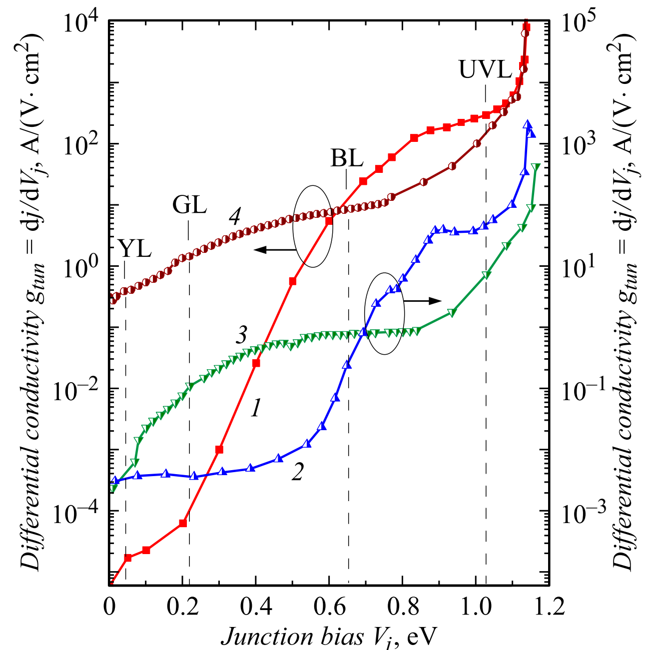

Figure 4. Differential conductivity as function of forward bias of Schottky barrier for Ni/*n*-GaN diodes A, B, C and D: A (*1*), B (*2*), C (*3*), D (*4*). The markers indicate the biases V_j at which the Fermi level F intersects the centers responsible for the peak energies of the YL, GL, BL and UVL PL bands in GaN.

approaches $V_j = 0.6$ eV growth g_{tun} for diodes C and D slows down, forming a plateau on the curves $\lg g_{tun}(V_j)$, and for diodes A and B the exponential increase is observed g_{tun}, and near $V_j \approx 0.6$ eV g_{tun} for diodes A and D and diodes B and C become equal. At $V_j > 0.6$ eV the plateau on the curves $\lg g_{tun}(V_j)$ is observed for diodes A and B, while for diodes C and D thge exponential increase is observed g_{tun}, so that when approaching $V_j = 1.2$ eV g_{tun} for diodes A and D, and diodes B and C again become almost equal.

The nature of the curves $g_{tun}(V_j)$ indicates a significant difference in the density of deeply localized states in impurity bands in diodes with Schottky barriers on *n*-GaN grown by the MOCVD method (diodes A and B) and HVPE (diodes C and D), with low and high tunnel conductivity at low biases, respectively. $g_{tun}(V_j)$ curves have a clearly defined structure, which is comparable to the main bands of intracenter photoluminescence and optical absorption in GaN according to data published in [12,13,21–27].

At the Schottky barrier height $V_0 = 1.2$ eV (p. 2), the energy distance between the top of the valence band and the Fermi level at the Ni/GaN interface at zero bias is approximately $F - E_v \approx E_g - V_0 \approx 2.22$ eV (band gap GaN $E_g = 3.42$ eV at $T = 300$ K). The threshold nature of the increase in forward current near zero bias, in the interval $V_j = 0-0.2$ eV, observed in Schottky diodes (Fig. 1, curves *1-4*) and reaching 3 orders of magnitude in the diode C (curve *3*), indicates the increase in the density of localized states at the level E_t with V_j increasing and corresponds to the threshold energy of optical absorption $h\nu_{th}$YL-centers responsible for yellow (YL) PL with peak emission energy $h\nu_p = h\nu_{th} = 2.2$ eV close to the energy difference $E_g - V_0 \approx 2.22$ eV. This suggests that at zero bias the Fermi level crosses the low-energy edge of the Gaussian band of YL-centers. In this case, the bias interval $V_j = 0.2-0.6$ eV, in which increase of $g_{tun}(V_j)$ is observed in diodes C and D (Fig. 4, curves *3, 4*), and the magnitude of the bias $V_j = 0.4$ eV, near which a slowdown in growth g_{tun} is observed, correspond to the threshold optical energy $h\nu_{th}$ and the maximum Gaussian of GL-centers responsible for green (GL) PL ($h\nu_{th} = h\nu_p = 2.4$ eV, $E_{0i} = 2.6$ eV). The results obtained indicate a predominance of defects responsible for YL and GL-PL in C and D diodes, which is in agreement with the bright yellow-green PL observed in bulk *n*- GaN grown by the HVPE method [23,19].

Exponential growth $g_{tun}(V_j)$ in diodes A and B (curves *1, 2*) as the bias approaches $V_j = 0.65$ eV and the subsequent decrease in the slope of the curves $\lg g_{tun}(V_j)$ near $V_j = 0.8$ eV can be associated with an increase in the tunneling flux of electrons thermally excited to energy equal to the maximum of the Gaussian centers responsible for blue (BL) PL ($h\nu_p = h\nu_{th} = 2.85$ eV, $E_{0i} = 3.05$ eV), and a subsequent decrease in the tunneling permeability of the effective barrier as a result of charge exchange. The appearance of a double maximum of the tunneling current in diodes B in the bias range $V_j = 0.6-1.05$ eV (curve *2*) is explained by the competing influence of the exponential increase in the density of states of the Urbach tail $\rho_{Uf}(E_t)$ at the level E_t and a decrease in the tunneling permeability and density of states on the high-energy wing of the BL Gaussian. A sharp increase in $g_{tun}(V_j)$ at biases $V_j > 1.05$ eV corresponds to the level E_t crossing the zone of UVL centers responsible for UV (UVL) PL ($h\nu_p = 3.25$ eV). The results obtained suggest a predominance in diodes A and B of defects with localization energies corresponding to BL and UVL centers, which correlates with the threshold energies of strong optical absorption bands close to the peak energies of BL and UVL PL characteristic for doped epilayers. *n*-GaN grown by MOCVD [13,24].

3.4. Tunneling through localized states in reverse direction

Deep centers with ionization energy $V_0 > E_i > F$ increase the equilibrium bulk charge density in the SCR of the Schottky barrier, promoting the concentration of the electric field near the Schottky contact. With reverse bias, the width of the SCR increases as a result of shielding the field of the external potential difference. Free electrons are drawn out the SCR by the electric field, as well as electrons thermally excited into the conduction band from deep centers, as a result of which the total bulk charge of ionized shallow donors and deep centers increases (Fig. 3, *d*). As the bulk charge increases with increase in reverse bias, the field strength in the near-contact layer increases, which leads to the increase in its tunneling permeability and, accordingly, to increase in the tunneling reverse current.

When the SCR expands with increase in reverse bias to the coordinate x, at which the high-energy edge of the ionized states of the Gaussian band $\rho_{Gi}(E)$ descends on the energy scale to the Fermi level in the neutral region and crosses it at bias $V = V_i$, the bulk charge density in the SCR $N^+(x)$ sharply decreases by qN^+_{Gi} (3). Since in the near-contact layer $F_b = (qN^+(V + V_0/q)/\varepsilon\varepsilon_0)^{1/2}$, at $V > V_i$ the field strength near the Schottky contact increases with increase in displacement more slowly than at $V < V_i$. As the reverse bias increases, and the contribution of deep Gaussian zones to the total space charge density $qN^+(x)$ gradually decreases, the increase in field strength in the near-contact layer slows down with increase in bias, and changes in the field strength at voltages V_i become weaker due to decrease in the relative contribution of shallower Gaussian bands to the total space charge. As a result, with increase in reverse bias, $\lg j(V)$ curves become more flat and smoother up to pre-breakdown reverse biases.

Conclusion

The stepwise appearance of CVC $\lg j(V)$ with forward bias of Ni/*n*-GaN Schottky barriers is due to the thinning of the barrier near the Schottky contact due to the bulk charge of deep localized states of defects in the band gap GaN, ionized in the field of the contact difference of potentials

and increasing the built-in electric field at the contact. The bulk charge of deep centers stimulates electron tunneling through the barrier along localized states of defects and reduces the effective barrier height E_{eff} to the energy of the Gaussian maximum of the impurity band at the Schottky interface $E_{0i}(x = 0) = E_{\text{eff}}$. During forward bias the main tunnel current is created by electrons thermally activated to energy at the Gaussian maximum, and is characterized by perfection factor close to unity. Recharging of the states of the Gaussian band with increase in bias causes the plateau appearance on CVC. During reverse bias the increase in the bulk charge causes thinning of the barrier in the near-contact layer, which stimulates the excess tunneling current of electrons, thermally activated to the effective barrier height $E_{\text{eff}} = E_{0i}(x = 0)$, from the metal through the near-contact layer, followed by electron drift in the bulk charge field.

Conflict of interest

The authors declare that they have no conflict of interest.

References

[1] Y. Sun, X. Kang, Y. Zheng, J. Lu, X. Tian, K. Wei, H. Wu, W. Wang, X. Liu, G. Zhang. Electronics, **8**, 575 (2019). DOI: 10.3390/electronics8050575

[2] R. Chu. Appl. Phys. Lett., **116**, 090502 (2020). DOI: 10.1063/1.5133718

[3] R.C. Sharma, R. Nandal, N. Tanwar, R. Yadav, J. Bhardwaj, A. Verma. J. Physics: Conf. Ser., **2426**, 012008 (2023). DOI: 10.1088/1742-6596/2426/1/012008

[4] H. Morkoç. *Handbook of Nitride Semiconductors and Devices* (Weinheim: WILEY-VCH Verlag GmbH & Co. KGaA, 2008), v. 2, p. 24.

[5] D. Yan, J. Jiao, J. Ren, G. Yang, X. Gu. J. Appl. Phys., **114**, 144511 (2013). DOI: 10.1063/1.4824296

[6] Y. Wang, H. Xu, S. Alur, Y, Sharma, F. Tong, P. Gartland, T. Issacs-Smith, C. Ahyi, J. Williams, M. Park, G. Wheeler, M. Johnson, A.A. Allerman, A. Hanser, T. Paskova, E.A. Preble, K.R. Evans. Phys. Stat. Sol. (c), **8** (7–8), 2430 (2011). DOI: 10.1002/pssc.201001158

[7] H. Hasegawa, M. Akazawa. J. Korean Phys. Soc., **55**, 1167 (2009).

[8] P. Reddy, S. Washiyama, F. Kaess, M.H. Breckenridge, L.H. Hernandez-Balderrama, B.B. Haidet, D. Alden, A. Franke, B. Sarkar, E. Kohn, R. Collazo, Z. Sitar. J. Appl. Phys., **119**, 145702 (2016). DOI: 10.1063/1.4945775

[9] S.Y. Karpov, D.A. Zakheim, W.V. Lundin, A.V. Sakharov, E.E. Zavarin, P.N. Brunkov, E.Y. Lundina, A.F. Tsatsulnikov. Semicond. Sci. Technol., **33**, 025009 (2018). DOI: /10.1088/1361-6641/aaa603

[10] E.V. Kalinina, N.I. Kuznetsov, V.A. Dmitriev, K.G. Irvine, C.H. Carter. J. Electron. Mat., **25** (5), 831 (1996). DOI: 10.1007/BF02666644

[11] A. Kumar, M. Latzel, S. Christiansen, V. Kumar, R. Singh. Appl. Phys. Lett., **107**, 093502 (2015). DOI: 10.1063/1.4929829

[12] C.H. Qiu, C. Hoggatt, W. Melton, M.W. Leksono, J.I. Pankove. Appl. Phys. Lett., **66** (20), 2712 (1995). DOI: 10.1063/1.113497

[13] O. Ambacher, W. Reiger, P. Ansmann, H. Angerer, T.D. Moustakas, M. Stutzmann. Sol. St. Commun., **97** (5), 365 (1996). DOI: 10.1016/0038-1098(95)00658-3

[14] P. Perlin, M. Osinski, P.G. Eliseev, V.A. Smagley, J. Mu, M. Banas, P. Sartori. Appl. Phys. Lett., **69** (12), 1680 (1996).

[15] J.R. Lang, N.G. Young, R.M. Farrell, Y.R. Wu, J.S. Speck. Appl. Phys. Lett., **101**, 181105 (2012).

[16] H. Zhang, E.J. Miller, E.T. Yu. J. Appl. Phys., **99**, 023703 (2006).

[17] X.M. Shen, D.G. Zhao, Z.S. Liu, Z.F. Hu, H. Yang, J.W. Liang. Sol. St. Electron., **49**, 847 (2005). DOI: 10.1016/j.sse.2005.02.003

[18] R.X. Wang, S.J. Xu, S.L. Shi, C.D. Beling, S. Fung, D.G. Zhao, H. Yang, X.M. Tao. Appl. Phys. Lett., **89**, 143505 (2006).

[19] V. Voronenkov, N. Bochkareva, R. Gorbunov, P. Latyshev, Y. Lelikov, Y. Rebane, A. Tsyuk, A. Zubrilov, Y. Shreter. Jpn. J. Appl. Phys., **52**, 08JE14 (2013). DOI: 10.7567/JJAP.52.08JE14

[20] *Tunneling Phenomena in Solids*, ed. E. Burstain, S. Lundqvist (Plenium Press, NY., 1969)

[21] S. Nakamura, G. Fasol. *The Blue Laser Diode: GaN Based Light Emitters and Lasers* (Springer, Berlin, NY., 1998), 343 p.

[22] S.F. Chichibu, A. Uedono, K. Kojima, H. Ikeda, K. Fujito, S. Takashima, M. Edo, K. Ueno, S. Ishibashi. J. Appl. Phys., **123**, 161413 (2018). DOI: 10.1063/1.5030645

[23] M.A. Reshchikov. Appl. Phys., **129**, 121101 (2021). DOI: 10.1063/5.0041608

[24] S.F. Chichibu, Y. Kawakami, T. Sota. in *Introduction to Nitride Semiconductor Blue Lasers and Light Emitting Diodes*, ed. by. S. Nakamura, S.F. Chichibu (Taylor & Francis, L., NY., 2000), ch. 5.

[25] N.I. Bochkareva, I.A. Sheremet, Yu.G. Shreter. Semiconductors, **50** (10),1369 (2016). DOI: 0.1134/S1063782616100109

[26] N.I. Bochkareva, Y.G. Shreter. Physics Solid State, **64** (3), 371 (2022). DOI: 10.21883/PSS.2022.03.53193.241

[27] N.I. Bochkareva, A.M. Ivanov, A.V. Klochkov, Y.G. Shreter. J. Phys.: Conf. Ser., 1697, 012203 (2020). DOI: 10.1088/1742-6596/1697/1/012203

[28] P.B. Klein, S.C. Binari. J. Phys.: Condens. Matter, **15**, R1641 (2003). DOI: 10.1088/0953-8984/15/44/R01

[29] R.J. Molnar, T. Lei, T.D. Moustakas. Appl. Phys. Lett., **62** (1), 72 (1993).

[30] D. Monroe. Phys. Rev. Lett., **54** (2), 146 (1985). DOI: 10.1103/PhysRevLett.54.146

[31] M. Nichus, R. Schwarz. Phys. Stat. Sol. (c), **3** (6), 1637 (2006). DOI: 10.1002/pssc.200565463

[32] A.G. Chynoweth, W.L. Feldmann, R.A. Logan. Phys. Rev., **121** (3), 684 (1961).

[33] L.V. Keldysh. ZhETF, **33** (4), 994 (1957); 34 (4), 962 (1958).(in Russian).

[34] N. Moulin, M. Amara, F. Mandorio, M. Limiti. J. Appl. Phys., **126**, 033105 (2019). DOI: 10.1063/1.5104314

Translated by I.Mazurov